Hindawi
International Journal of Photoenergy
Volume 2018, Article ID 7082785, 5 pages
https://doi.org/10.1155/2018/7082785

Research Article

Synthesis of $MgFe_2O_4$/Reduced Graphene Oxide Composite and Its Visible-Light Photocatalytic Performance for Organic Pollution

Fengmin Wu, Wenlu Duan, Mei Li, and Hang Xu

School of Chemical Engineering and Pharmaceutics, Henan University of Science and Technology, Luoyang 471023, China

Correspondence should be addressed to Hang Xu; xhinbj@126.com

Received 1 February 2018; Revised 18 July 2018; Accepted 6 August 2018; Published 26 August 2018

Academic Editor: P. Davide Cozzoli

Recently, binary metal oxides have been proven to be the most investigated semiconductors due to their high activity for the removal of organic pollutants. In this paper, to improve the photocatalytic efficiency of $MgFe_2O_4$, a $MgFe_2O_4$/reduced graphene oxide (MFO/rGO) photocatalyst was synthesized by a facile generalized solvothermal method. The morphology, structure, and photocatalytic activities in the degradation of methyl orange (MO) reaction were systematically characterized by scanning electron microscopy, transmission electron microscopy, X-ray diffraction, and UV-vis absorption spectroscopy, respectively. The results showed that the MFO/rGO composite exhibited enhanced photocatalytic performance in the photodegradation of MO under visible-light irradiation and reached a maximum degradation rate of 99% within 60 min of irradiation. This excellent photocatalytic performance is attributed to the introduction of rGO in the composite, which can effectively reduce the photoproduction of the electron-hole pair recombination rate. The excellent photocatalytic activity reveals that the MFO/rGO composite photocatalyst is a promising photocatalyst with good visible-light response and has potential applications in the field of water treatment.

1. Introduction

Recently, environmental pollution has become one of the outstanding social problems. Photocatalytic technology has attracted great interest as a promising pathway for solving energy supply and environmental pollution problems [1, 2]. However, the traditional photocatalysts, typically TiO_2 (3.2 eV) or ZnO (3.3 eV), with a wide band gap can only exhibit excellent photocatalytic activity under ultraviolet light irradiation, which significantly limits their practical applications [3–5]. Faster kinetics recombination of photogenerated electrons and holes is another chief reason for lower photocatalytic performance [6]. It takes patience to develop efficient visible-light irradiation photocatalysts in order to utilize solar light, of which about 45% is composed of visible light. Thus, the development of visible-light photocatalysts has become one of the most critical topics in photocatalytical research today.

Magnesium ferrite ($MgFe_2O_4$, MFO) is a semiconductor with a spinel structure, which can absorb visible light due to its narrow band gap (approximately 2.0 eV) and is not sensitive to photoanodic corrosion. MFO has been used as a photocatalyst for the degradation of 2-propanol [7]. Besides, it was found that MFO/TiO_2 has a high photocatalytic activity for the degradation of the RhB contaminant [8]. Therefore, MFO is considered as one of the efficient photocatalyst candidates for air or water treatment. According to previous reports, to reduce the recombination of photogenerated electrons and holes, the surface of photocatalysts coated with carbon nanotubes (CNTs) or carbon nanofibers (CNFs) has been considered as a promising strategy [9]. In the process of photocatalysis, CNTs or CNFs can act as an excellent electron-acceptor/transport donor to effectively facilitate the migration of photoinduced electrons and hinder the quick recombination in electron transfer, which enhances photocatalytic performance.

As a rising star in the carbon family, reduced graphene oxide (rGO) has attracted a great deal of attention in recent years due to its excellent electronic properties (zero gap semiconductor where the conduction band and the valence band touch each other), outstanding ability as an electron acceptor and transport, chemical stability, and high surface area, which have been used to obtain hybrid materials with superior photocatalytic performance [10]. For instance, tremendous improvement has been reported for metal oxides [11], metal sulfides [12], and nonmetal g-C_3N_4 [13] by using rGO as a synergistic catalyst material. However, to the best of the authors' knowledge, there has been no report of the modification of MFO with rGO for preparing new photocatalysts.

In this paper, a novel MFO/rGO photocatalyst has been synthesized by a facile solvothermal method for the first time. The as-prepared samples were characterized, and the photocatalytic activity under visible-light irradiation ($\lambda \geq 420$ nm) was estimated by the photodegradation of methyl orange (MO). The results indicated that MFO/rGO nanocomposites exhibited much higher photocatalytic performance than the pure MFO. At last, the mechanism of enhanced photocatalytic activities of MFO/rGO is proposed.

2. Experimental

2.1. Catalyst Preparation. All reagents were of analytical grade and used without further purification. Commercial graphite power was used as the raw materials for synthesis of graphene oxide (GO) by a modified Hummer's method according to previous reports [14].

1.75 mmol of $Mg(NO_3)_2{\cdot}6H_2O$ and 3.5 mmol of $Fe(NO_3)_3{\cdot}9H_2O$ were mixed and dissolved in 80 ml of distilled water after being sonicated for 30 min. Next, a certain amount (10 ml) of 10 mg ml^{-1} GO suspension was added into the above solution under magnetic stirring for 4 h. The pH value of the solution was adjusted by ammonia hydroxide to about 10. The mixture was stirred vigorously for an hour and then sealed in a Teflon lined stainless steel autoclave (100 ml capacity). The autoclave was heated to and maintained at 180°C for 12 h, and allowed to cool to room temperature. The grayish-black products were washed several times with ethanol and distilled water, and then dried in a vacuum oven at 80°C overnight. For comparison, bare MFO was also synthesized by a similar route without adding the GO suspension.

2.2. Characterization. The morphology and structure of the as-prepared samples were characterized by a field-emission scanning electron microscope (FESEM, Hitachi S-4800) equipped with an energy-dispersive spectrometer (EDS, Bruker QUANTAX-400), high-resolution transmission electron microscope (HRTEM, Tecnai G2 F20), and X-ray diffractometer (XRD, Holland PaNalytical PRO PW3040/60) with Cu Kα radiation ($V = 30$ kV, $I = 25$ mA, $\lambda = 1.5418$ Å, scanning rate: 10° min^{-1}). UV-vis absorption spectra of samples were recorded on a UV-vis spectrophotometer (Hitachi U-3310) with a wavelength range of 200–600 nm.

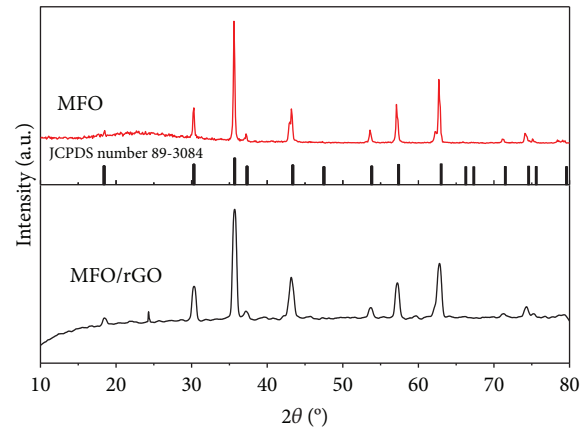

Figure 1: The XRD patterns of MFO and MFO/rGO samples.

2.3. Photocatalytic Tests. The photocatalytic performance was evaluated with the as-prepared sample powder (50 mg) suspended in MO (20 mg l^{-1}, 100 ml) with constant stirring. A 300 W Xe arc lamp (CEL-HXF 300, Beijing Jinyuan Co. Ltd.) was used as the light source and equipped with an ultraviolet cutoff filter to provide visible light ($\lambda \geq 420$ nm). Prior to irradiation, the suspensions were stirred in the dark for 30 min to ensure the adsorption/desorption equilibrium. At certain time intervals, 2 ml of the suspension was taken and centrifuged to remove the photocatalyst particles. The filtrate was then analyzed using a UV-vis spectrophotometer at 464 nm as a function of irradiation time by measuring the max absorbance of MO.

3. Results and Discussion

The XRD patterns of the products are shown in Figure 1. The dominant diffraction peaks in the pattern of MFO and MFO/rGO can be indexed to those from the spinel $MgFe_2O_4$ (JCDPS 89-3084). The diffraction peaks of the MFO are sharp and intense, revealing the highly crystalline character of the sample. After combination with rGO, the intensity of the diffraction peaks becomes weak. However, the crystalline spinel of the sample was not changed, indicating that the crystal structure of MFO remains stable. In addition, the characteristic diffraction peaks of GO (12.2°) are not found in the XRD of MFO/rGO composite samples, which indicates that GO is fully reduced to rGO during the process of reaction.

Figures 2(a) and 2(b) display the SEM images of the MFO and MFO/rGO samples. The MFO are composed of numerous hexahedron particles, each with a particle size of about 80 nm. The MFO/rGO shows ultrathin crumpled three dimensional (3D) nanosheets, and the MFO and GO are uniform and well-attached to each other. Figures 2(c) and 2(d) show the typical low-magnification TEM images of MFO/rGO, which indicate that the as-prepared material has a quadrangular morphology with the edge length in the range of 30–50 nm. Figures 2(e) and 2(f) show the high-resolution TEM images of MFO/rGO. The lattice spacing measured (Figure 2(f)) for the crystalline plane is 0.263 nm, corresponding to the (111) plane of the spinel MFO (JCPDS 89-

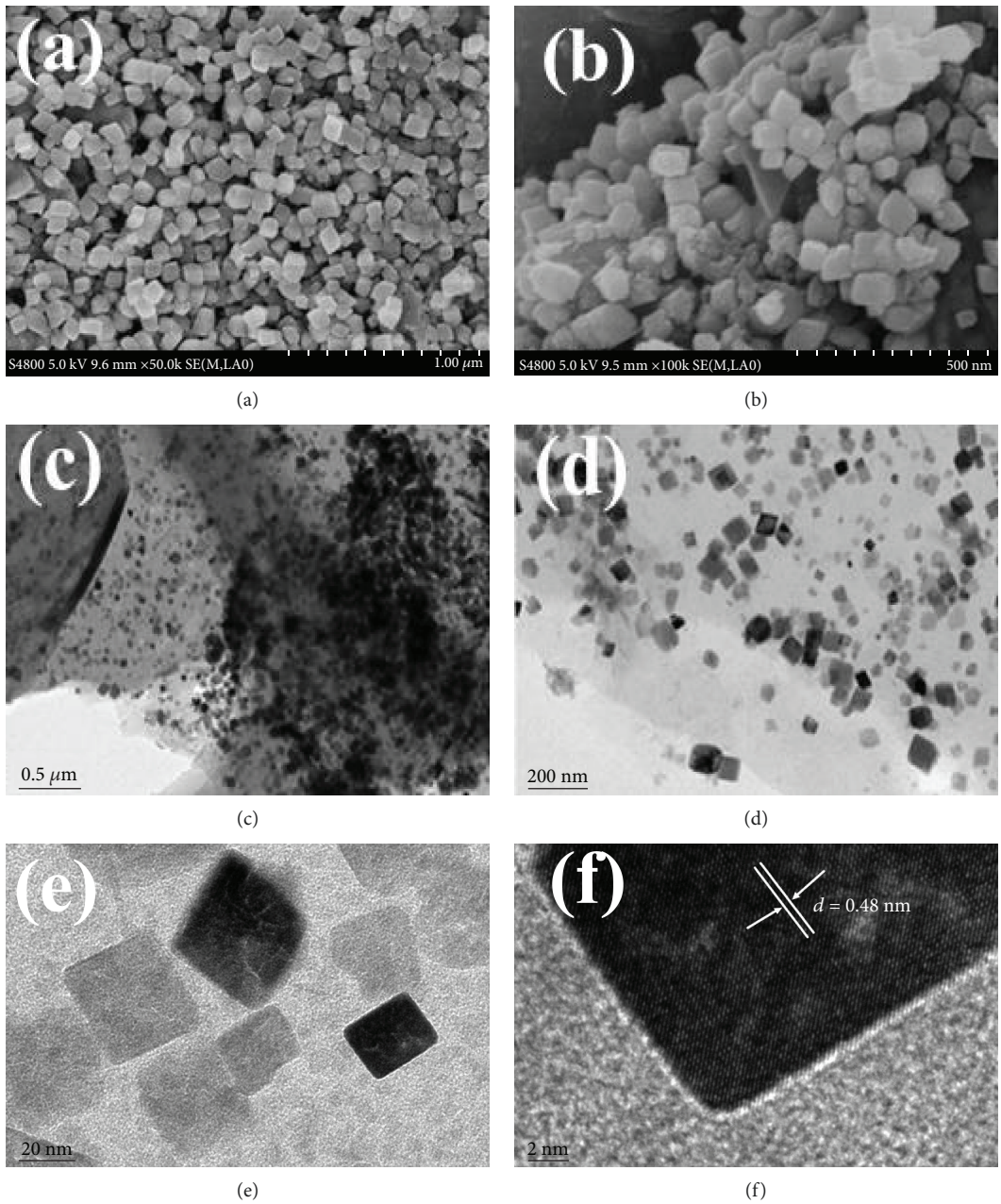

Figure 2: The SEM images of MFO (a) and MFO/rGO (b) and low-magnification (c, d) and high-resolution (e, f) TEM images of MFO/rGO.

3084). In addition, rGO serves as a 3D conductive support for MFO nanoparticles.

As can be seen from Figure 3(a), MO self-photodegradation (under light irradiation without the effect of catalysts) can be negligible; however, the MFO/rGO composite exhibits the best visible-light photocatalytic efficiency, which can decompose MO molecules in 60 min. In contrast, the MFO showed a poor degradation efficiency of ~40% after visible-light irradiation for 60 min. Interestingly, rGO also showed a degradation efficiency of about 20% owing to its absorbing ability to visible light [15]. Figure 3(b) shows the absorbance spectra of MO under rGO, MFO, and MFO/rGO photocatalysts at different times. The enhancement of the photocatalytic performance should be ascribed to the prevention in electron-hole pair quick recombination due to the stepwise energy level structure in the composite and the increase in the light absorption with the presence of rGO [16]. Therefore, on the basis of the synergistic effect of the electron-acceptor and transport material rGO and the rGO can absorb visible light, and the MFO/rGO composite displays a highly efficient visible-light photocatalytic activity.

The mechanism of the photocatalytic degradation of MO is given as follows: Firstly, the semiconductor materials (MFO) absorb the photon under light irradiation, and the electron-hole pairs are generated at the photocatalyst surface (1). Then, photoinduced electrons are transferred from the MFO to the rGO, which could efficiently separate the photogenerated electrons and hinder the charge recombination in

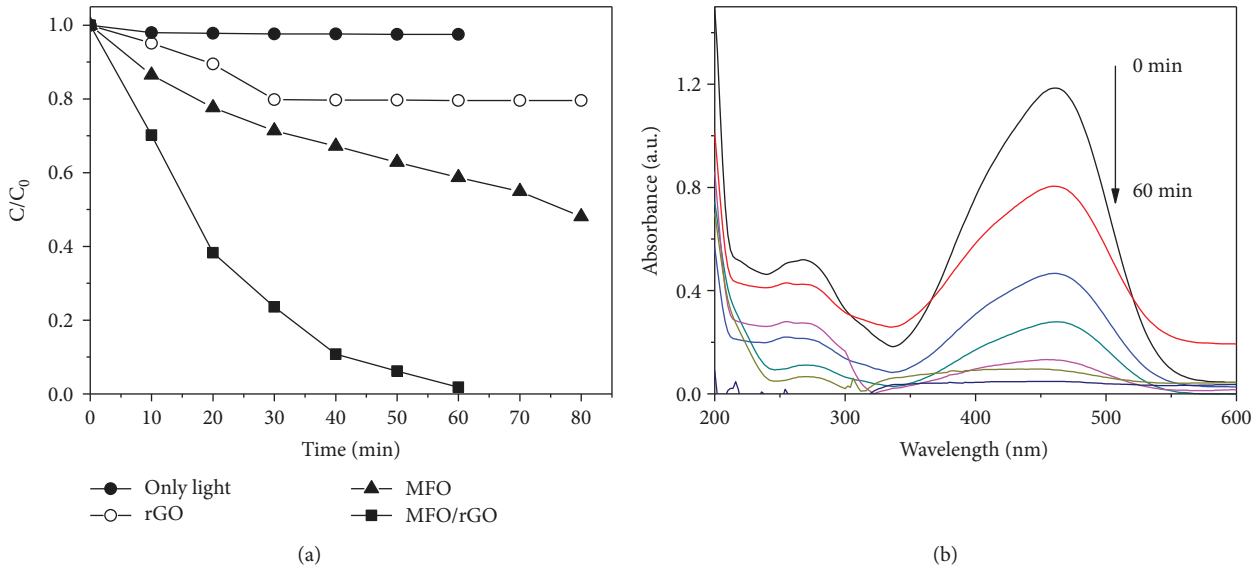

Figure 3: (a) Photocatalytic degradation profile of MO under visible-light irradiation with and without catalyst versus exposure time, (b) absorption spectra of the MO (20 mg l^{-1}) solution at different photocatalytic time under MFO/rGO photocatalytic.

the electron transfer processes. Afterwards, the high oxidation potential of the holes causes the direct oxidation of the MO and some reactive intermediates are generated (2). Finally, a hydroxyl radical can also be created by hydroxyl ions (OH^-) with holes (3). Furthermore, the superoxide anions are also formed by the molecular reduction of O_2, which may take place by the presence of electrons in the conduction band at the surface of the photocatalyst (4). The conduction band electrons are also responsible for the production of $^{\bullet}OH$ and $^{\bullet}O_2^-$, which have been identified as the main cause of MO degradation. Due to existence of rGO among MFO, which hinder the recombination of photogenerated electrons and holes, the photocatalytic performance is thus enhanced.

$$\mathrm{MFO} + h\nu \longrightarrow \mathrm{MFO} + e_{CB}^- + h_{VB}^+ \quad (1)$$

$$h_{VB}^+ + \mathrm{MO} \longrightarrow \mathrm{MO}^* + \text{oxidation of MO} \quad (2)$$

$$h_{VB}^+ + OH^- \longrightarrow {}^{\bullet}OH \quad (3)$$

$$e_{CB}^+ + O_2 \longrightarrow {}^{\bullet}O_2^- \quad (4)$$

4. Conclusion

In summary, a novel photocatalyst MFO/rGO composite was prepared via a facile generalized solvothermal method. The results demonstrate that the incorporation of rGO can enhance the photocatalytic activity for the degradation of MO. The reduced photogenerated electron-hole pair recombination and the enhanced visible-light absorbance with the introduction of rGO are mainly responsible for the enhanced photocatalytic activity of the MFO/rGO composite. The present synthetic strategy should be a promising fabrication technique for a simple, rapid, and effective method of the composite photocatalysts for the removal of organic pollutants.

Data Availability

The data used to support the findings of this study are available from the corresponding author upon request.

Conflicts of Interest

The authors declare that they have no conflicts of interest.

Acknowledgments

The work was supported by the National Natural Science Foundation of China (no. 21006075) and Henan Provincial Science and Technology Foundation (nos. 152102210274 and 15A530008).

References

[1] J. Mu, C. Shao, Z. Guo et al., "High photocatalytic activity of ZnO-carbon nanofiber heteroarchitectures," *ACS Applied Materials & Interfaces*, vol. 3, no. 2, pp. 590–596, 2011.

[2] M. R. Hoffmann, S. T. Martin, W. Choi, and D. W. Bahnemann, "Environmental applications of semiconductor photocatalysis," *Chemical Reviews*, vol. 95, no. 1, pp. 69–96, 1995.

[3] Z. Zheng, J. Zhao, Y. Yuan et al., "Tuning the surface structure of nitrogen-doped TiO_2 nanofibres—an effective method to enhance photocatalytic activities of visible-light-driven green synthesis and degradation," *Chemistry - A European Journal*, vol. 19, no. 18, pp. 5731–5741, 2013.

[4] X.-J. Lv, W.-F. Fu, H.-X. Chang et al., "Hydrogen evolution from water using semiconductor nanoparticle/graphene composite photocatalysts without noble metals," *Journal of Materials Chemistry*, vol. 22, no. 4, pp. 1539–1546, 2012.

[5] R. Huang, H. Ge, X. Lin et al., "Facile one-pot preparation of α-$SnWO_4$/reduced graphene oxide (RGO) nanocomposite with improved visible light photocatalytic activity and anode

performance for Li-ion batteries," *RSC Advances*, vol. 3, no. 4, pp. 1235–1242, 2013.

[6] R. M. Asmussen, M. Tian, and A. Chen, "A new approach to wastewater remediation based on bifunctional electrodes," *Environmental Science & Technology*, vol. 43, no. 13, pp. 5100–5105, 2009.

[7] H. G. Kim, P. H. Borse, J. S. Jang et al., "Fabrication of $CaFe_2O_4/MgFe_2O_4$ bulk heterojunction for enhanced visible light photocatalysis," *Chemical Communications*, no. 39, pp. 5889–5891, 2009.

[8] D.-H. Yoo, T. V. Cuong, V. H. Pham et al., "Enhanced photocatalytic activity of graphene oxide decorated on TiO_2 films under UV and visible irradiation," *Current Applied Physics*, vol. 11, no. 3, pp. 805–808, 2011.

[9] L.-P. Zhu, G.-H. Liao, W.-Y. Huang et al., "Preparation, characterization and photocatalytic properties of ZnO-coated multi-walled carbon nanotubes," *Materials Science and Engineering: B*, vol. 163, no. 3, pp. 194–198, 2009.

[10] J. Mu, B. Chen, M. Zhang et al., "Enhancement of the visible-light photocatalytic activity of In_2O_3-TiO_2 nanofiber heteroarchitectures," *ACS Applied Materials & Interfaces*, vol. 4, no. 1, pp. 424–430, 2012.

[11] K. Zhou, Y. Zhu, X. Yang, X. Jiang, and C. Li, "Preparation of graphene—TiO_2composites with enhanced photocatalytic activity," *New Journal of Chemistry*, vol. 35, no. 2, pp. 353–359, 2011.

[12] S. Min and G. Lu, "Sites for high efficient photocatalytic hydrogen evolution on a limited-layered MoS_2 cocatalyst confined on graphene sheets—the role of graphene," *Journal of Physical Chemistry C*, vol. 116, no. 48, pp. 25415–25424, 2012.

[13] Q. Xiang, J. Yu, and M. Jaroniec, "Preparation and enhanced visible-light photocatalytic H_2-production activity of graphene/C_3N_4 composites," *Journal of Physical Chemistry C*, vol. 115, no. 15, pp. 7355–7363, 2011.

[14] D. C. Marcano, D. V. Kosynkin, J. M. Berlin et al., "Improved synthesis of graphene oxide," *ACS Nano*, vol. 4, no. 8, pp. 4806–4814, 2010.

[15] X. He, T. Tang, F. Liu, N. Tang, X. Li, and Y. Du, "Photochemical doping of graphene oxide thin film with nitrogen for photoconductivity enhancement," *Carbon*, vol. 94, pp. 1037–1043, 2015.

[16] X. An, J. C. Yu, Y. Wang, Y. Hu, X. Yu, and G. Zhang, "WO_3 nanorods/graphene nanocomposites for high-efficiency visible-light-driven photocatalysis and NO_2 gas sensing," *Journal of Materials Chemistry*, vol. 22, no. 17, pp. 8525–8531, 2012.